Optics Letters

Optically formed rubbery waveguide interconnects

Georgios Violakis,[1] Athanasios Bogris,[1,2] Stergios Pispas,[3] George Fytas,[1,4] Benoit Loppinet,[1] and Stavros Pissadakis[1,*]

[1]Foundation for Research and Technology-Hellas (FORTH), Institute of Electronic Structure and Laser (IESL), 70013, Heraklion, Greece
[2]Department of Materials Science & Technology, University of Crete, 70013, Heraklion, Greece
[3]National Hellenic Research Foundation (NHRF), Theoretical and Physical Chemistry Institute (TPCI), 11635 Athens, Greece
[4]Max Planck Institute for Polymer Research, 55128 Mainz, Germany
*Corresponding author: pissas@iesl.forth.gr

Received 23 June 2021; revised 1 October 2021; accepted 6 October 2021; posted 8 October 2021 (Doc. ID 435052); published 28 October 2021

Light induced self-written waveguides (LISWs) with unique elongation characteristics and low optical loss are formed in a monodispersed polyisoprene solution using a low-power laser photopolymerization process, while their light transmission characteristics are exemplified in the flexible interconnection of two single-mode optical fibers operating in the visible/near infrared wavelengths. The LISWs formed exhibit rubbery properties, allowing extensibilities upon cases from 400% to 800%, while still retaining significant optical transmission. The rubber elasticity enables sustaining LISWs at stressed lengths longer than 500 μm propagation losses from 1.0 to 2.9 dB/mm.

https://doi.org/10.1364/OL.435052

Soft matter photonics has garnered great attention due to their potential to drive a number of devices with unmatched mechanical, biochemical, and optical properties for application in the emerging fields of wearable sensors [1,2] and modular optics [3,4], where the scale of the physical deformation can significantly vary with respect to the actual dimensions of the device. The development of elastic, stand-alone waveguide interconnects, especially between optical fibers, can inaugurate a new type of optical component that combines high integration characteristics with better transmission than the free-space propagation, yet facilitating relaxed linking tolerances. Optical fiber interconnects, where the waveguide bridge is formed through a self-written fabrication, exhibit practical impact. Focusing on the last point, light induced self-written waveguides (LISWs) constitute a particular type of light-guiding element inside a photosensitive medium [5]. The propagation of a laser beam simultaneously records a waveguide under modal evolution conditions that departs from the free-space propagation [6]. LISWs have been demonstrated in transient or permanent mode and in solid, liquid, and gaseous optical media, using several recording laser sources and exposure conditions. There have been efforts to produce organic-based, self-arranged photonic devices by employing multi-compound single-photon [7,8] or two-photon photopolymerizable materials [9]. This technology has found its way into applications for the connection of two misaligned optical waveguides [10] and for self-repairing strain sensors [11].

Here, we demonstrate the connection of two single-mode optical fibers with a new type of rubbery self-written waveguide joints. The material consists of an entangled polymer solution activated by a low-power continuous-wave (CW) red laser. The single-photon fabrication of rubbery waveguides up to 500-μm-long is achieved and simultaneously maintains high optical transmission and enables elongations from 400% to 800%. The propagation characteristics of these elastic LISWs can be easily controlled by tuning exposure time and using a few mW visible CW laser beam. The fabrication conditions appear promising for implementing these propagation characteristics into real applications. The propagation losses of these waveguides were found to be as low as 1.0 dB/mm for short range links (up to 250 μm), reaching 2.9 dB/mm for links up to 500 μm.

The material used for the formation of the rubbery waveguides is a 5 wt % semi-dilute solution of monodispersed 1090 kDa polyisoprene (PI) in decane. This is known to produce self-written structures under laser irradiation at 671 nm in the mW range [12] but none at wavelengths ≥700 nm [13]. The solution was placed inside a 1 × 1 × 10 mm square borosilicate glass capillary cell with both sides open and placed on the setup depicted in Fig. 1. A CW diode laser at 671 nm and output power of ∼20 mW was used as the waveguide formation light source. Another non-writing probe beam of a 780 nm CW diode laser was used for system alignment and monitoring of the elastic LISW transmission during formation. Typical power output of the probe laser was ∼1.5 mW, measured at the feeding optical fiber. Both lasers were coupled into an optical fiber wavelength coupler, and its output port was coupled to an optical fiber (SM600 Fibercore, single mode at 671 nm) with a core radius of ∼2.0 μm and a cladding diameter of 125 μm. Both SM600 optical fibers were clamped using V-grooves and inserted inside the polymer solution, opposite side in the cuvette (see Fig. S1 Supplement 1). The 671 nm laser output at the SM600 optical fiber was ∼7.8 mW. The relative positioning

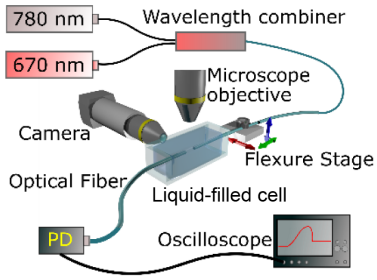

Fig. 1. Experimental setup for the creation and performance monitoring of the rubbery waveguide joint between two single-mode optical fibers.

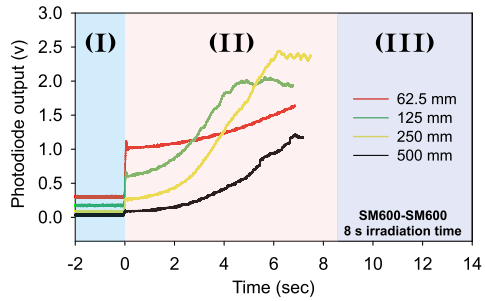

Fig. 2. Optical signal evolution during LISW formation as a function of recording time for four fiber-to-fiber distances (62.5–500 μm). Section I, 780 nm light only; Section II, 780 nm (probe) + 671 nm (inscription) light; and Section III, 780 nm light only.

of the two fibers was performed using 2-axis, 20× microscope objectives coupled to CCD cameras. The two fiber end-faces were further aligned by maximizing the transmission of the probe laser, which was measured using a photodiode (PD). The distance between the two end-faces was varied between 15 and 500 μm. The PD signal was monitored during the writing process, allowing optimization of the LISW recording time. The coupling efficiency, $\eta = P_{out}/P_{in}$, between the two SM600 optical fibers was estimated from the power probe light, reaching the photodiode at the end of the receiving fiber and the light measured at the exit of the incoming SM600 optical fiber at 780 nm.

The LISW light recording process, as a function of time, was divided into three temporal sections, as presented in Fig. 2. First, in Section I the two SM600 fibers were aligned at a given distance and light coupling efficiency was maximized, defining the reference level of the probe laser. Then the writing laser (671 nm) was turned on, resulting in an increase of the signals at the PD. In Section II, the overall signal is seen to increase as a result of the writing process reaching a maximum after few seconds. After approximately 8 s, the writing laser was turned off, and the transmission of the probed laser was monitored and found to be stable (Section III). The discontinuities observed at $t = 0$ s and $t \sim 8$ s are due to switching the 671 nm laser writing beam on and off. Since absorption at the recording and probe wavelengths are considered minimum [13], we anticipate that changes in the coupling efficiency during recording are attributed to modal field diameter and scattering losses.

The recording of the LISWs was also monitored using the microscope objectives, which shows the size of the LISW and proved the absence of bending or misshaping. Snapshots of

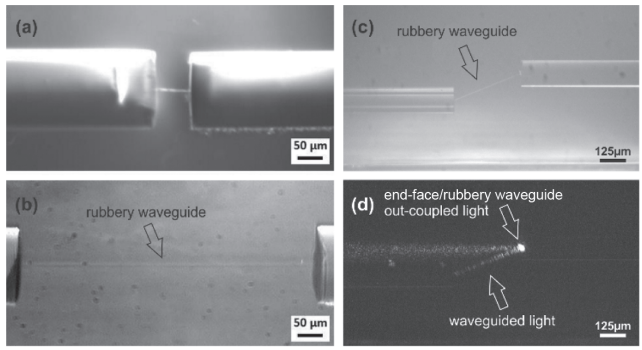

Fig. 3. (a), (b) Optical microscopy photos of unstrained LISWs formed between SM600 optical fibers placed at different distances. (c) Bright and (d) dark field optical microscopy photos of a 320-μm-long LISW, laterally misaligned while resulting in angular displacement of the LISW [14] with respect to the SM600 optical fiber axis of ∼22°. The transmission of the misaligned system is ≤2% due to light launching beyond the acceptance angle of the LISW and out-coupling at the fiber end (bright scattering is from the 780 nm laser).

the resulting LISWs are shown in Fig. 3 for different distances between the fiber end-faces. The chosen LISW exposures (∼8 s) were found to maximize the probe beam transmission. Longer exposures formed LISWs of lower η, as a large increase of light scattering rendered degraded transmission. Shorter irradiations were found to form mechanically unstable LISWs of lower optical transmission (see Fig. S2 in Supplement 1). All LISWs tested intact for the duration of the experiments (up to one day) without measurable mechanical or optical degradation. LISWs up to 125-μm-long proved stable over weeks, and longer length LISWs tended to detach from the SM600 end-face.

The coupling efficiency measured after the writing process, as a function of distance between fiber end-faces, is shown in Fig. 4. For LISW lengths up to 250 μm, η was close to 80%, while it dropped down to ∼55% for longer (∼500 μm) connections (black circles in Fig. 4). Formation of LISWs longer than 500 μm was possible but required longer exposures in the given PI solution at the cost of poorer optical performance. The formed LISWs offer transmittances of up to 4× times larger than those of the free-space propagation. The coupling efficiencies estimated for the LISW interconnections exhibit a reasonable agreement with experimental and theoretical values for the non-connected fibers (see data in Fig. 4). The LISW interconnect transmission was confirmed in broadband spectral measurements, which was obtained by using low-power white light from a tungsten source (Fig. 5). No spectral rippling, associated with multi-modal beating, was observed, and this supported the assumption of single-mode operation. Overall, losses of the LISW interconnect are expected to emerge from light scattering by geometrical defects such as shape or refractive index (RI) inhomogeneity. In addition, mode field mismatch losses due to refractive index mismatch at the SM600-LISW interfaces can impact the transmittance. The latter losses can be estimated by knowing the diameter and the RI of the LISWs.

The temporal evolution of the LISW diameter and the RI were estimated using quantitative phase contrast optical microscopy on a separate setup in the absence of the receiving fiber [15]. The SM600 fiber was used for phase contrast calibration. Figure 6(a) illustrates the temporal evolution of the phase image

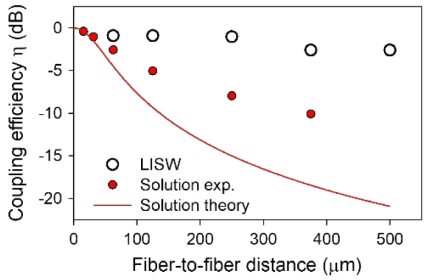

Fig. 4. Coupling efficiency (η) of a LISW formed in the PI solution; experimental (red points) and theoretical (red line) data. (Due to unstripped cladding guidance, the coupling is slightly larger than the open space propagation in the PI solution.)

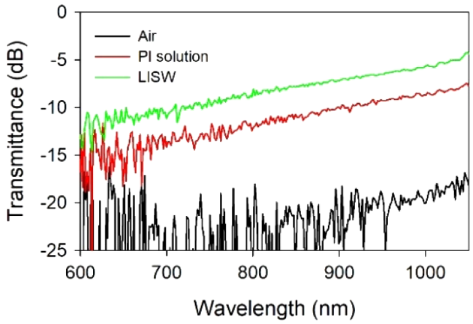

Fig. 5. Transmission spectra (green line) of a LISW interconnect formed between two SM600 fibers, spaced at 125 μm apart and for an exposure of 9 s, inside the PI solution. Transmission of the SM600 fiber system in air (black) and in the polyisoprene (PI) solution (red).

upon irradiation. The refractive index contrast was increasing with irradiation time, while the LISW diameter was almost constant. A LISW with a core radius of 2 μm became visible after a ∼4 s laser exposure, and longer exposures (10 s) led to a slightly larger radius (less than 10% increase). The experimental RI increase, as a function of irradiation time, is shown in Fig. 6(b). The LISWs exhibited a RI contrast of $\sim 3 \times 10^{-2}$ after a 30 s exposure, which amounts to ∼50 mJ and can be compared to the PI-solution RI $n_{sol} = 1.416$ and RI of bulk PI $n_{PI} = 1.52$.

For the specific recording conditions of the LISWs, the main source of mode-mismatch-related loss is expected to originate from RI changes. The mode field diameter (MFD) mismatch loss between the LISW and the SM600 optical fiber can be estimated knowing the LISW radius and RI time evolution [Fig. 6(b)]. The photorecording process is of single-photon nature [16], which asserts a linear correspondence between the modal size of the SM600 fiber and the LISW. We further assumed a homogenous RI profile [17], using mode coupling theory for circular, weakly guided waveguides to evaluate the modal profile of the LISWs (Eq. S1 Supplement 1). The same approach was used for the case of the SM600 fiber, assuming a numerical aperture (NA) of 0.12. For short irradiation times (≤6 s), the RI of the LISW leads to a −0.3 dB MFD mismatch loss per junction. However, as the irradiation time increases to 10 s and the RI locally increases, the MFD mismatch losses rise to −0.81 dB. The estimation of the MFD mismatch losses further helps elucidate the basic figure of LISW transmission attenuation deduced from the measured transmission efficiency. For the 8 s exposure case (Fig. 4), and up to 250 μm LISW links,

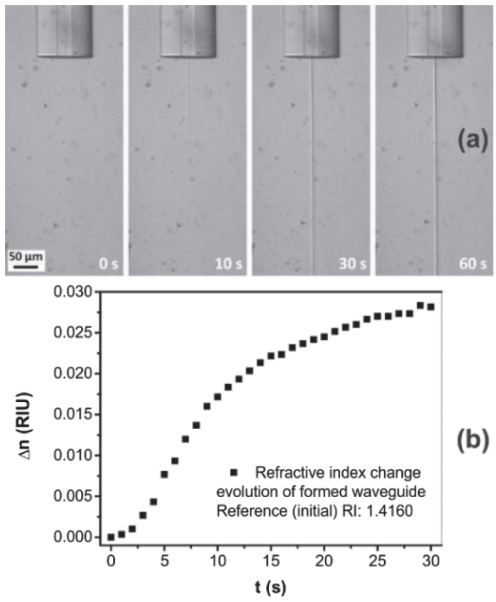

Fig. 6. (a) Optical microscope snapshots of LISW formation for different time instances during a single exposure. (b) Refractive index increase of a single-ended LISW versus irradiation time at ∼10 mW.

total fiber-to-fiber losses are ∼ − 0.97 dB so that a propagation loss of ∼0.27 dB is projected (accounting total MFD = 14%), which is equivalent to 1.08 dB/mm. For LISWs of lengths up to 500 μm, the transmission losses substantially increase above 3.0 dB/cm. This may be related to modal field distortion due to prolonged propagation inside the LISW length [8], which degrades the quality of the waveguide recording process. Additionally, rubbery LISWs formed between far apart spaced optical fibers (larger than 250 μm) are particularly prone to additional bending and distortion losses and core-to-core alignment imperfections between the two SM600 optical fibers.

The used polyisoprene semi-dilute solution exhibits rubbery viscoelasticity and finds its origin in entangled polymer chains. However, it is a transient elasticity, as the materials eventually flows. The LISWs are expected to preserve rubber elasticity but make it permanent, as the writing process leads to the formation of irreversible crosslinks. In fact, the latter enables the realization of stretchable waveguides. To verify this behavior, we tested the optical performance of the LISWs as a function of tensile elongation. A 62.5 μm LISW was formed with an irradiation time of 10 s. This slightly longer than the optimal exposure time (see Fig. 2) was used to improve the rigidity of the LISW. The coupling efficiency measured for this LISW is ∼1.54 dB (70%). The translation stage (Fig. 1) was used to increase the distance between the two SM600 fibers and thereby to stretch the LISW. The transmission of the probe laser was measured as a function of the elongation of the rubbery LISW. During elongation, the LISW was still immersed in the PI/hexane solution. Transmission signal intensities, normalized to that measured before strain exertion, are presented in Fig. 7 versus optical fiber-to-fiber distance. The specific rubbery LISW was stretched up to a length of 300 μm, reaching an impressive 4.8× increase of its initial length before detaching from the landing optical fiber end-face. For comparison, characteristic elongation figures of other elastomer-based waveguides are of the order of 30% [18]. For elongations up to 50% (from 62.5 to 90 μm),

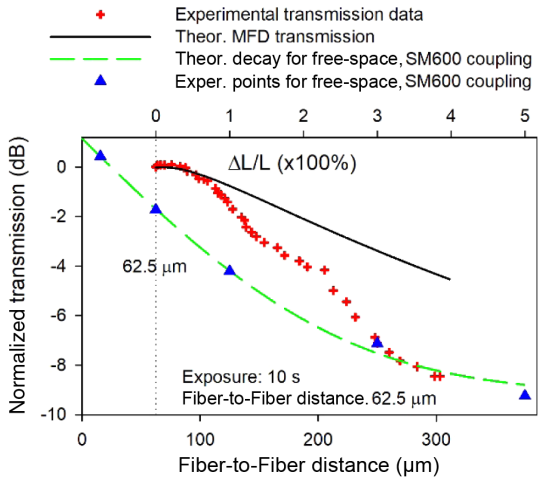

Fig. 7. Normalized transmission of a LISW under stretch as a function of SM600 optical fibers distance (red crosses). All data are normalized to the power of the 780 nm signal for the LISW at 62.5 μm. The solid black line refers to transmission, accounting solely for the MFD coupling between the SM600/LISW junctions. The blue triangle points refer to the experimentally measured free-space coupling between the SM600 optical fibers still immersed in the PI solution. The green dashed line is the theoretical exponential decay.

the optical performance of the LISW does not deteriorate; the contrary shows a slightly increased relative transmission. It is likely that both micro-bending losses are removed, and strain contraction better matches the modal profile of the LISW with the SM600 fibers. For elongations up to 100%, a gradual loss increase of 1.55 dB is recorded with further stretching up to 200% length increase, introducing total losses of ∼4 dB. Up to a ∼4-fold extension (250 μm) the rubbery joint is still waveguiding, albeit only marginally better than the free-space propagation for optical fibers being immersed in the same PI solution. Beyond 250 μm, the probe light seems to mostly leak outside the LISW, similar to the guidance observed in a thin optical fiber taper. By assuming a Poisson ratio of 0.5 for the rubbery PI-based LISW [19] and a 4× elongation figure, the actual LISW diameter contracts down from 2 to ∼1.0 μm. The last leads to a single-mode (LP_{01}) propagation and a corresponding modal confinement of the order of 8% at 780 nm (for comparison, nominal modal confinement of SM600 is ∼75% at 780 nm). The LISW modal confinement number is estimated without accounting for possible photoelastic changes occurring in the stretched waveguide core. Photoelastic refractive index changes, occurring along the axis of propagation, will further suppress the modal confinement.

The strain-induced contraction of the transverse dimension of the LISW is also expected to increase mode coupling losses of the LISW with the SM600 fibers. Above 4× LISW elongation, total mode coupling losses reach ∼4.4 dB (64%). An important observation emerging from Fig. 7 is related to the actual loss mechanisms involved during the elongation of the LISWs. For small elongations, the MFD losses rather dominate, while for extended elongations, due to modal leakage from the LISW, overall losses resemble those of free-space propagation. LISWs recorded using longer exposure conditions (12 s) have been stretched up to elongation ratios of 8.6× while still maintaining significant optical transmission (∼ − 8 dB) above the free-space propagation limit (see Fig. S3 in Supplement 1). Full shape and optical transmission recovery of the strained LISWs was possible up to extensions of ≤2×. Larger extensions introduced plasticity changes as "rope-like" deformation of the recovered LISW. For example, a 6× extended LISW, after relaxed to its initial length, was subjected to 4 dB total losses. Also, LISWs recorded using multi-mode optical fibers exhibited significantly higher modal beating and propagation losses.

Our work showed the possibility of realizing extremely elastic, light induced self-written waveguides with extensibilities up to 800% and intrinsic waveguide losses as low as 1.0 dB/mm while using a low-power, red CW laser. The optical and mechanical performance of these LISWs and their fabrication paves the way for long-length elastic optical interconnects, adjustable power couplers, and wearable sensors. Rubbery LISWs are expected for most polydienes dispersed in a great variety of solvents. This variability allows optimization of the formulation for better connection, including tuning of the refractive index for lower MFD losses and Young's modulus through control of the crosslink density. Our studies are now focused on the light repairing functionalities of those LISWs.

Funding. European Research Council (694977); H2020 Industrial Leadership (779472, ACTPHAST 4.0); Laserlab-Europe (871124).

Disclosures. The authors declare no conflicts of interest.

Data Availability. Data underlying the results presented in this paper are not publicly available at this time but may be obtained from the authors upon reasonable request.

Supplemental document. See Supplement 1 for supporting content.

REFERENCES

1. J. Guo, C. Yang, Q. Dai, and L. Kong, Sensors (Basel) **19**, 3771 (2019).
2. A. Candiani, M. Konstantaki, A. Pamvouxoglou, and S. Pissadakis, IEEE J. Sel. Top. Quantum Electron. **23**, 210 (2017).
3. A. Stefani, S. C. Fleming, and B. T. Kuhlmey, APL Photon. **3**, 051708 (2018).
4. G. Panusa, Y. Pu, J. Wang, C. Moser, and D. Psaltis, Opt. Mater. Express **9**, 128 (2019).
5. M. Kagami, T. Yamashita, and H. Ito, Appl. Phys. Lett. **79**, 1079 (2001).
6. A. S. Kewitsch and A. Yariv, Opt. Lett. **21**, 24 (1996).
7. C. Ecoffet and D. J. Lougnot, J. Lightwave Technol. **28**, 1278 (2010).
8. R. Malallah, D. Cassidy, I. Muniraj, J. P. Ryle, J. J. Healy, and J. T. Sheridan, Appl. Opt. **57**, E80 (2018).
9. S. Jradi, O. Soppera, and D. J. Lougnot, Appl. Opt. **47**, 3987 (2008).
10. T. Yoshimura, M. Iida, and H. Nawata, Opt. Lett. **39**, 3496 (2014).
11. Y. J. Song and K. J. Peters, Smart Mater. Struct. **20**, 065005 (2011).
12. R. Sigel, G. Fytas, N. Vainos, S. Pispas, and N. Hadjichristidis, Science **297**, 67 (2002).
13. M. Anyfantakis, A. Königer, S. Pispas, W. Köhler, H.-J. Butt, B. Loppinet, and G. Fytas, Soft Matter **8**, 2382 (2012).
14. A. Günther, S. Schneider, M. Rezem, Y. Wang, U. Gleissner, T. Hanemann, L. Overmeyer, E. Reithmeier, M. Rahlves, and B. Roth, J. Lightwave Technol. **35**, 2678 (2017).
15. A. Roberts, E. Ampem-Lassen, A. Barty, K. A. Nugent, G. W. Baxter, N. M. Dragomir, and S. T. Huntington, Opt. Lett. **27**, 2061 (2002).
16. M. Anyfantakis, B. Loppinet, G. Fytas, and S. Pispas, Opt. Lett. **33**, 2839 (2008).
17. D. Marcuse, Bell Syst. Tech. J. **56**, 703 (1977).
18. J. Missinne, S. Kalathimekkad, B. Van Hoe, E. Bosman, J. Vanfleteren, and G. Van Steenberge, Opt. Express **22**, 4168 (2014).
19. G. N. Greaves, A. L. Greer, R. S. Lakes, and T. Rouxel, Nat. Mater. **10**, 823 (2011).